Interpretation of Amide I Difference Bands Observed during Protein Reactions Using Site-Directed Isotopically Labeled Bacteriorhodopsin as a Model System†

Karin Hauser,[#] Martin Engelhard,[‡] Noga Friedman,[§] Mordechai Sheves,[§] and Friedrich Siebert*,[#]

AG Biophysik, Institut für Molekulare Medizin und Zellforschung, Albert-Ludwigs-Universität Freiburg, 79104 Freiburg, Germany, Max-Planck-Institut für Molekulare Physiologie, 44227 Dortmund, Germany, and Department of Organic Chemistry, Weizman Institute of Science, Rehovot 76100, Israel

Received: July 30, 2001

Reaction-induced infrared difference spectra show characteristic amide I spectral changes, which indicate conformational changes of the protein backbone but which cannot be interpreted at a molecular level. To obtain some insights into their causes, we used bacteriorhodopsin as a model system and investigated its BR → N transition during which the largest amide I changes are observed. For the molecular interpretation, we labeled a single peptide C═O group at specific positions of the backbone with ^{13}C and monitored the resulting isotope effects. This has been achieved by replacing specific amino acids with a cysteine. Because wild-type bacteriorhodopsin does not contain this amino acid, (1-^{13}C)cysteine can be incorporated into the mutants for site-directed isotopic labeling. Although the isotope-induced spectral changes are very small, we observed clear isotope effects for the middle to extracellular part of helices B, C, and F, indicating that the backbone of these parts of the protein is distorted during the reaction, whereas no label effects could be identified for the E−F loop and for the cytosolic regions of helices E and F. The results are discussed within the framework of recent experimental and theoretical studies of the amide I band, and they are correlated to the structural changes observed by other methods.

Introduction

Conformational changes of proteins during their activity are functionally important for the reaction mechanism. In reaction-induced infrared difference spectroscopy, characteristic bands attributed to such conformational changes are observed in the amide regions. They are thought to arise from small alterations in the protein backbone. However, a molecular interpretation of these difference bands is not yet possible. They are mainly interpreted only in a qualitative way as indicators for small backbone changes that have occurred during the reaction of the protein. Secondary structure elements of peptides and proteins can be distinguished in infrared absorption spectra by the typical frequencies of their amide I absorption bands representing mainly the carbonyl stretching vibration of the peptide groups. In recent years, there have been a large number of theoretical and experimental studies on the origin of the sensitivity of the amide I band to the secondary structure. They include empirical force-field calculations of peptides and proteins,[1] quantum chemical calculations on the amide I mode of small peptides,[2,3] and experimental and theoretical studies on the influence of ^{13}C-labeling of the C═O group of one or several peptide bonds in well-defined peptides.[4−7] In all studies involving more than one peptide group, the importance of the transition dipole coupling (TDC) has been emphasized for the determination of the amide I frequency. It represents an electrostatic coupling of the individual amide I oscillators similar to a vibrational excitonic system. In a recent publication, it has been shown that the amide I band of proteins can be well described by a single amide I oscillator frequency and the inclusion of the transition dipole coupling.[8] Infrared intensities have been calculated by the application of the 3D-doorway model commonly used for excitonic systems.[9,10] This allows the determination of the contribution of each peptide group to the different parts of the broad amide I absorption band. Furthermore, the system of coupled amide oscillators of small peptides has been studied by nonlinear-infrared spectroscopy.[11,12] Such investigations provide information on the coupling of the different oscillators and on their dynamics and therefore form the molecular basis for the understanding of the amide modes. If it were possible to combine them with reaction-induced difference spectroscopy, detailed molecular information on the accompanying structural changes of the backbone could be deduced. However, reactions of native proteins usually do not involve changes of the secondary structure. It is generally thought that in the transition from one state to another during a protein reaction the backbone structure is only slightly modified: small changes in the dihedral angle may take place along with changes in hydrogen bonding of the C═O peptide groups as well as changes in the mutual orientation of the amide I oscillators. Furthermore, protein reactions may involve more global structural changes including small rearrangements of secondary structural elements, that is, tilting, twisting, and distance changes.

It is a common feature of reaction-induced difference amide I bands that they are rather narrow in contrast to the normal absorption bands of peptides and proteins. Tilting of secondary structural elements would cause broad intensity changes in orientated samples due to the polarization dependence of the

† Part of the special issue "Mitsuo Tasumi Festschrift".

* To whom correspondence should be addressed. Telephone: +49-761-2035396. Fax: +49-761-2035399 or +49-761-2035390. E-mail: frisi@uni-freiburg.de.

[#] Albert-Ludwigs-Universität Freiburg.

[‡] Max-Planck-Institut für Molekulare Physiologie.

[§] Weizman Institute of Science.

10.1021/jp012926e CCC: $22.00
Published on Web 01/18/2002

TABLE 1: Positions of the Cysteine and Thus of the Isotopically Labeled Peptide Group within the Secondary Structure of Bacteriorhodopsin

residue	position
T46	helix B (middle region)
L93	helix C (middle region)
F154	helix E (cytoplasmic side)
S162	Loop EF
S169	helix F (cytoplasmic side)
A184	helix F (middle to extracellular side)

amide modes. Thus, we can expect that the narrow amide I difference bands rather reflect local distortions of the secondary structure. However, the influence of such distortions on the amide modes has not yet been theoretically treated.

Some insights on the effect of local distortions may be gained from the experimental and theoretical studies using site-specific ^{13}C isotope labels at one or a few neighboring peptide groups. This causes a frequency downshift of the corresponding local oscillators, comparable to a drastic change in hydrogen bonding of the respective C═O groups. Furthermore, detuning the oscillator frequencies drastically alters the coupling behavior, which is additionally influenced by changes in the orientation of the transition moments, that is, by changes in the orientation of the peptide groups. Therefore, it appears possible to gain some basic insights from such isotopic labeling studies for the molecular interpretation of the amide difference bands.

Whereas static and time-resolved Fourier transform infrared (FTIR) difference spectroscopies are established as powerful methods for the study of molecular changes of amino acid side chains (especially carboxyl groups, aromatic amino acids, histidines), and of cofactors (e.g., chromophores, substrates),[13] the changes of amide modes during protein reactions have so far eluded a molecular interpretation.

In this article, we report on the interpretation of amide I spectral changes identified by FTIR difference spectra during protein reactions. Site-directed isotope labeling of specific peptide groups in the protein backbone has been used as a tool for the interpretation. As a model system, we used the photoreaction of the light-driven proton pump bacteriorhodopsin (BR), a membrane protein containing the seven transmembrane α-helices A−G. Photon absorption by light-adapted BR initiates a photocycle passing through the successive photointermediates J, K, L, M, N, and O, which are characterized by their absorption maxima in the visible spectral region, their lifetimes, the isomerization and protonation state of the chromophore, the protonation state of internal aspartic acids, and the protein conformation (for reviews see refs 14 and 15). Because wild-type BR contains no cysteines, site-directed labeling could be realized by the introduction of [1-^{13}C]Cys into site-directed cysteine mutants. In addition, the structure of bacteriorhodopsin's dark state is known[16−20] and thus the secondary structure element containing this specific cysteine residue. If a label effect can be identified in the infrared difference spectra, its spectral position can be compared to the amide I frequency of the corresponding unlabeled, secondary structural element. Six mutants (see Table 1) have been investigated allowing isotopic labeling of peptide groups located at different positions in the structure. An obvious prerequisite to see any isotope-induced changes in the difference spectra is that the labeled peptide group undergoes structural changes in the respective intermediate or that it is vibrationally coupled to a peptide region undergoing corresponding alterations. It should be mentioned that the effects of ^{13}C isotopic labeling of a C═O group(s) of the bacteriorhodopsin backbone on difference spectra have been studied before by either explicit site-directed isotope labeling[21,22] or labeling all amino acids belonging to one species.[23] Here, we will demonstrate that if the label position is close to the middle or extracellular side of the helices, clear spectral changes could be identified in the BR → N difference spectra, whereas label positions at the cytoplasmic end or in the EF loop cause, if any, much smaller spectral changes, which could not be resolved. The BR → N transition has been chosen because in the corresponding difference spectrum the largest amide I bands are observed. Our results show that site-directed isotopic labeling can be used to localize distortions of secondary structural elements occurring during protein reactions. However, because the spectral changes partially occur at frequency positions not characteristic for the respective secondary structure, the nature of the structural changes cannot be directly deduced and the molecular interpretation awaits further theoretical studies.

Materials and Methods.

Sample Preparation. The methods for obtaining the cysteine mutants of bacteriorhodopsin[24] and for incorporating labeled amino acids[25] have been described earlier. The incorporation of ^{13}C-cysteine was more than 60%. The all-*trans*-9-demethyl-retinal analogue (9H-retinal) was synthesized according to published schemes.[26,27] The BR-cysteine mutants were bleached and reconstituted with the retinal analogue as described.[28,29] Film samples were prepared using the isopotential spin-dry centrifugation technique.[30] The centrifugation cells were developed for a vacuum ultracentrifuge (L60 Beckman Instruments, Munich, Germany) and a SW28 swinging bucket rotor. To allow evaporation of the solvent, a small hole was introduced in the bucket cap (diameter 0.5 mm) and a phosphorus-bronze pinhole (diameter 0.1 mm) was fixed over the hole. A volume of 70 μl of protein solution with 100 μg BR was centrifuged on a AgCl window with 50 000 g (20 °C, 4 h 30 min). For sufficient photometric accuracy in the amide I spectral change, rehydration of the protein films was controlled to achieve a transmission at 1650 cm^{-1} of about 20%.

Spectroscopy. Time-resolved rapid scan measurements were performed with a Bruker ifs88 spectrometer and a photovoltaic MCT detector (Kolmar) showing good linearity. The sample was light-adapted for 5 min with light of wavelengths >495 nm. Sample temperature was 18 °C. The samples were excited at 520 nm by an excimer laser-pumped dye laser (Lamda Physik). Spectral resolution was 8 cm^{-1}. To improve the signal-to-noise ratio, each measurement has been repeated between 64 and 128 times and the resulting difference spectra have been averaged. Measurement conditions are annotated under each figure.

Results

Experimental Considerations. Because different samples (labeled and unlabeled protein) have to be compared, reproducibility of sample preparation and measurement conditions is a necessary prerequisite for the analysis of the amide bands. This is especially critical because, as it will be shown below, the observed spectral differences are very small. The intensities and frequency positions of the amide difference bands are sensitively influenced by several parameters being discussed below. Different degrees of orientation of the purple membranes on the sample window evoke variations in infrared intensities in the amide I region.[31] The Lambert−Beer law is only valid for homogeneous samples, that is, for samples of which the concentration does not vary over the area. Therefore, if this condition is not met, the relative intensity of bands in the

difference spectra will vary depending on the homogeneity. To control both conditions, well-orientated and homogeneous protein film samples have been prepared by the isopotential spin-dry centrifugation technique.[30]

The largest isotope-induced spectral changes are expected for difference spectra between those states of the photoreaction in which the largest amide I difference bands are observed. For the photoreaction of bacteriorhodopsin, these occur in the transition to the N state. However, this intermediate is difficult to obtain in pure form and the admixture of other states greatly varies depending on external parameters such as temperature, pH, and humidity. Humidity could be only reproducibly controlled by overlaying the membrane film with a thin layer of water and by sealing this "sandwich" sample with a second window. However, this results in a very low transmission (less than 10%) in the amide I spectral range due to the strong water absorbance, inhibiting the reliable determination of the size of the amide difference bands. Overlaying the film with ^2H_2O instead of H_2O would increase the transmission, but the variability of H/^{2}H exchange of the peptide groups, influencing both the position and the intensity of amide I difference bands, caused considerable variations in the spectra. Therefore, the protein film samples have been hydrated via the water vapor phase, the extent of hydration being controlled by the Fermi resonance band at 2250 cm^{-1}.

To still be able to reliably measure the BR → N difference spectra, we took advantage of the fact that by reconstituting bacterioopsin (the protein without the chromophore) with all-*trans*-9H-retinal (a retinal analogue in which the 9-methyl group has been removed), the photocycle is slowed about 250-fold and is characterized by a long-lived N-like intermediate[32] in which large amide I spectral changes occur. Therefore, the mutants were reconstituted with all-*trans*-9H-retinal. In the case of the L93C-mutant, we exploited the fact that this mutant has a slowed-down photocycle with a long-lived, red-shifted, but still N-like, intermediate accumulating after release and re-uptake of protons.[33,34] The slowed-down photocycles allow time-resolved measurements in the rapid-scan mode.

Analysis of the Amide I Difference Bands and Data Evaluation. Typical for the amide regions of protein difference spectra are several narrow bands spread over the whole amide frequency region. These amide difference bands are caused by parts of the protein backbone undergoing conformational changes during the protein reaction. It is not completely clear how isotopic labeling of a single peptide oscillator will influence the amide difference bands. The simplest case would be the original difference band being replaced by a shifted band. For an isolated amide I oscillator, a frequency shift of 37 cm^{-1} is expected when the ^{12}C atom is exchanged by a ^{13}C atom.[35] However, this pattern is complicated by the coupling of the amide I oscillators, which depends on the local secondary structure as well as on the strength of the H bonds, lowering the C═O bond strength. Thus, the labeling may cause more complex spectral changes. To better resolve them, the difference spectra of the labeled and the unlabeled protein are subtracted and the "double" difference spectrum is obtained. Difference bands not influenced by the isotopic label should cancel in the double difference spectrum, whereas changes in intensity, frequency, and band shape evoke double difference bands. For normalization of the difference spectra, the fingerprint bands of the chromophore between 1300 cm^{-1} and 1100 cm^{-1} have been used, being characteristic of a definite photointermediate state. A necessary prerequisite is that difference spectra of the same intermediates are compared. Otherwise changes in the amide difference bands are evoked because of varying intermediate compositions. For the 9H-BR mutants, this was controlled by comparing subsequent spectra in the data block of the N-like states: if the differences vanish in the noise, such spectra are selected and co-added to improve the signal/noise ratio. Therefore, the extracted time domain, and thus the number of averaged spectra during the rapid-scan measurement, is different for each mutant depending on the kinetics of the respective photocycle.

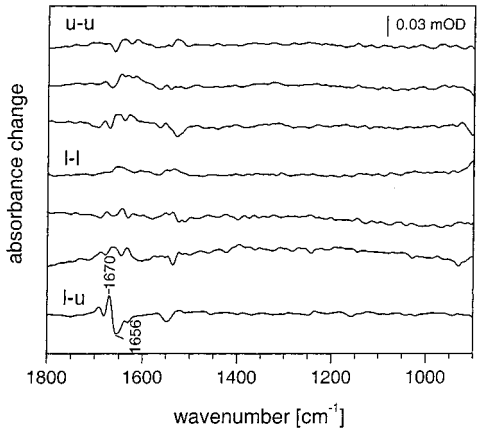

Figure 1. Subtraction of BR → N difference spectra of 9H-^{13}C-T46C and 9H-T46C (18 °C in H_2O with no buffer at 1.35−4.24 s after laser excitation). The double differences between 9H-T46C difference spectra (u−u, spectra 1−3 from the top) and between 9H-^{13}C-T46C difference spectra (l−l, spectra 4−6 from the top) reveal small bands almost of the same magnitude as the isotope-induced bands in the double difference spectrum of 9H-^{13}C-T46C and 9H-T46C (l−u).

Though the preparation of the film samples has been optimized (see Experimental Considerations), small bands are still observed in the double difference spectra not caused by the isotopic labeling. This becomes evident when double difference spectra are formed between two spectra of different samples of the same type (either both labeled or both unlabeled). The origin of these bands is not completely clear. They are not due to instrumental errors and not due to noise. It might be that they are caused by remaining variations in the sample preparation. Also, the normalization procedure for subtracting the unlabeled from the labeled difference spectrum probably may contribute to these bands because the chromophore bands are used for normalization under the assumption that a well-defined chromophore state corresponds to a well-defined protein state. However, we observed that the amide I difference bands show small variations, although the chromophore bands do not differ. They might be caused by small variations in the level of hydration of the different samples, which is difficult to control at the desired accuracy. The difficulty to distinguish between these bands and the isotope-induced bands is demonstrated in Figure 1, where differences between spectra of the same type (unlabeled−unlabeled (u−u) or labeled−labeled (l−l)) are compared with the isotope-induced difference (l−u).

To minimize the spectral differences described above that are not caused by the isotopic labeling, several samples of each mutant have been prepared and several measurements have been performed. If measurements have been repeated with the same sample, it has been dried and rehydrated each time. Averaging of the resulting spectra partly compensates these differences and additionally reduces the noise. Another attempt to reduce these differences has been performed by applying the mathematical method of the singular value decomposition (SVD) to the measured data.[36] A matrix of several measured difference spectra

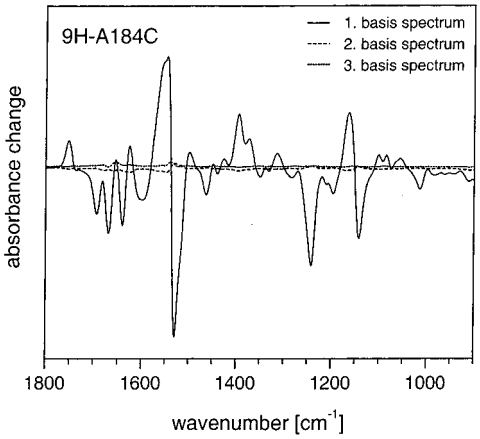

Figure 2. Singular value decomposition (SVD) of the BR → N difference spectrum of 9H-A184C (18 °C in H_2O with no buffer at 0.96−4.49 s after laser excitation). SVD has been performed with a data set of eight difference spectra (measured with two samples). The first three basis spectra are shown (first basis spectrum (solid line), second basis spectrum (dashed line), third basis spectrum (dotted line)). Generally, the double difference spectrum was formed with the first basis spectrum of the unlabeled and labeled samples, respectively. The software Matlab (The Math Works Inc.) was used for applying the SVD method.

is decomposed into eigenvectors by this method, and therefore, the difference spectrum is described as a linear sum of weighted factors (here called basis spectra). The weighting is represented by the singular values representing the square roots of the eigenvalues. This method is capable of resolving the common features of the difference spectra and of separating them from statistical and nonstatistical variations. This is typically demonstrated in Figure 2. The difference spectrum representing the N state of 9H-A184C has been analyzed. Eight spectra measured with two samples have been used. The first basis spectrum includes the main part of the difference spectrum (singular value $= 1.36 \times 10^{-2}$), whereas the second and third basis spectra represent eigenvectors with significantly smaller singular values (1.6×10^{-3}; 3×10^{-4}). Generally, the double difference spectrum was then formed with the first basis spectrum of the unlabeled and labeled samples, respectively. Both procedures for data evaluation, simple averaging of several spectra and singular value decomposition, have been applied, and the resulting double difference spectra have been compared. If both procedures yielded the same results, the identification of isotope-induced bands was considered to be reliable.

Identification of Isotope Effects in the N-Like States of the Various Samples Labeled at Specific Sites. *9H-T46C.* Threonine 46 is located in the middle region of helix B. The BR → N difference spectra of 9H-T46C and 9H-^{13}C-T46C together with the double difference spectrum are shown in Figure 3. SVD has been performed with a data set of seven difference spectra of 9H-T46C (measured with one sample) and five difference spectra of 9H-^{13}C-T46C (measured with two samples). The difference spectra in Figure 3 are the respective first basis spectra taken to form the double difference. Simple averaging of the data has provided essentially the same results. Comparison of both difference spectra reveals intensity changes in the amide I region. This can be seen more clearly in the double difference spectrum. The reproducibility of the N photointermediate in the various spectra is indicated by the flat baseline between 1300 and 1100 cm^{-1}. Double difference bands are only observed in the amide regions. The positive band at 1670 cm^{-1} and the negative band at 1656 cm^{-1} represent clear isotope-induced spectral changes, whereas the shoulders at 1692

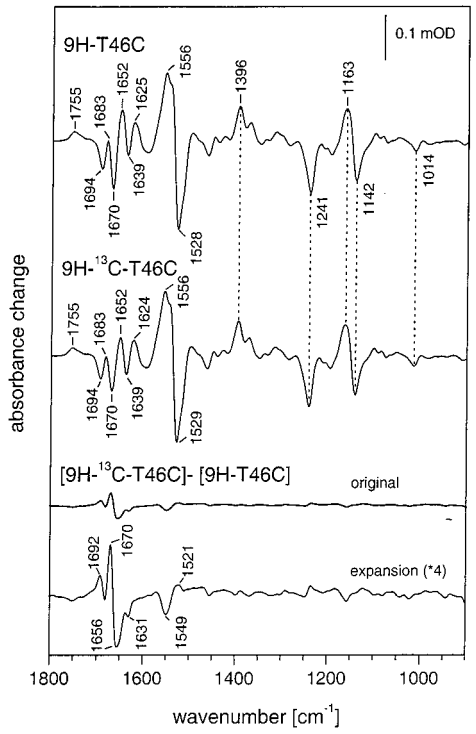

Figure 3. BR → N difference spectra of 9H-^{13}C-T46C and 9H-T46C (18 °C in H_2O with no buffer at 1.35−4.24 s after laser excitation). SVD has been performed with a data set of five difference spectra of 9H-^{13}C-T46C (measured with two samples) and seven difference spectra of 9H-T46C (measured with one sample). The shown difference spectra represent the resulting first basis spectra and have been used to form the double difference. The double difference spectrum is shown in original size and four times expanded.

cm^{-1} and at 1631 cm^{-1} as well as the changes in the amide II region at 1549 and 1521 cm^{-1} are very small and their significance is difficult to judge. It is important to note that this ^{13}C labeling will also induce a downshift of an isolated amide II oscillator.

L93C. Leucine 93 is located in the middle region of helix C. In comparison to that of wildtype-BR, the photocycle of L93 mutants is slowed and characterized by a long-lived red-shifted intermediate, which accumulates after the release and uptake of protons but before the reisomerization of the retinal to its initial all-*trans* state.[37] In Figure 4, difference spectra of L93C and ^{13}C-L93C together with the double difference spectra are shown for different time domains representing an N-like intermediate (0−0.01 s), which decays in the red-shifted intermediate (0.15−0.35 s). The very similar amide I bands indicate that the protein conformation has not changed as compared to the earlier N-like state. The large reduction of the negative band at 1535 cm^{-1}, which represents the ethylenic stretching vibration of the chromophore, indicates that this photoproduct has a visible absorption maximum very similar to the initial state.[38−40] Both intermediates are characterized by fingerprint IR bands of the chromophore at 1187 cm^{-1} (+), 1164 cm^{-1} (−), 1395 cm^{-1} (+), and 1301 cm^{-1} (+), which are typical for the 13-cis isomerization of the retinal.[41] A data set of 11 difference spectra of L93C (measured with two samples) and 12 difference spectra of ^{13}C-L93C (measured with two samples) has been used for SVD. The difference spectra in Figure 4 are the respective first basis spectra taken to form the double difference. Simple averaging of the data has provided essentially the same results. Comparison of the double difference spectra of N and the red-shifted intermediate essentially shows the same

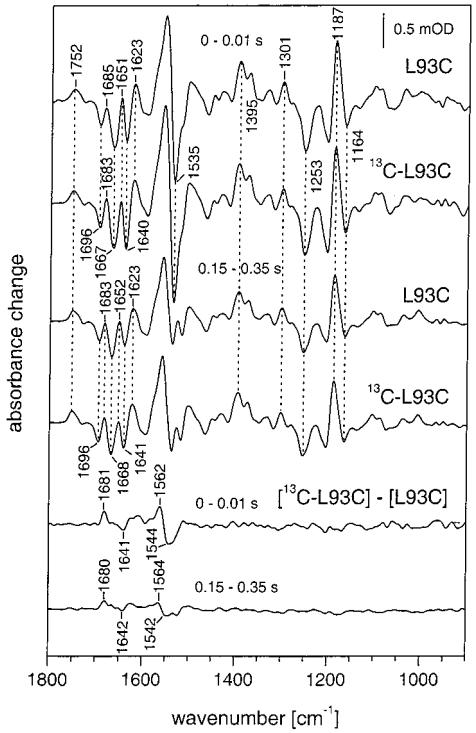

Figure 4. Difference spectra of ^{13}C-L93C and L93C (18 °C in H_2O with no buffer). The N-like intermediate (0−0.01 s after laser excitation) decays in the red-shifted intermediate (0.15−0.35 s after laser excitation). SVD has been performed with a data set of 12 difference spectra of ^{13}C−L93C (measured with two samples) and 11 difference spectra of L93C (measured with two samples). The shown difference spectra represent the resulting first basis spectra and have been used to form the double difference.

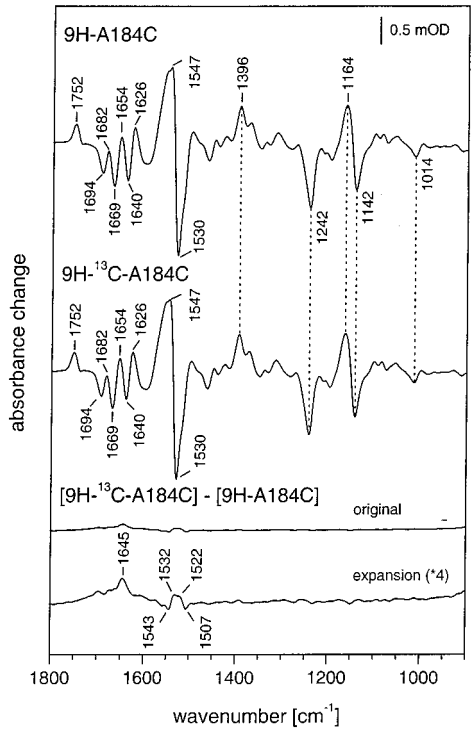

Figure 5. BR → N difference spectra of 9H-^{13}C-A184C and 9H-A184C (18 °C in H_2O with no buffer at 0.9−4.43 s after laser excitation). SVD has been performed with a data set of 11 difference spectra of 9H-^{13}C-A184C (measured with three samples) and eight difference spectra of 9H-A184C (measured with two samples). The shown difference spectra represent the resulting first basis spectra and have been used to form the double difference. The double difference spectrum is shown in original size and four times expanded.

isotope-induced band patterns. This confirms that the band changes in the difference spectra are mainly evoked by the chromophore, whereas the protein backbone is not substantially altered during the transition of N to the red-shifted intermediate. The positive band at 1681 cm^{-1} (+) and the negative band at 1641 cm^{-1} (−) observed in the double difference for the N state undergo small frequency shifts to 1680 and 1642 cm^{-1}, respectively. Significant bands are additionally observed in the amide II region at 1562 cm^{-1} (+)/1544 cm^{-1} (−) in N and at 1564 cm^{-1} (+)/1542 cm^{-1} (−) in the red-shifted intermediate, demonstrating that the same features are again conserved. This is especially remarkable because the observed position of the amide II bands might be altered by the strong ethylenic mode of the chomophore absorbing in the same frequency region. The short time domain of 12 ms in the N spectra explains the poorer signal-to-noise ratio compared to the red-shifted intermediate.

9H-A184C. Alanine 184 is located in the middle to extracellular region of helix F. The difference spectra of 9H-^{13}C-A184C and 9H-A184C together with the double difference spectrum are shown in Figure 5. A data set of eight difference spectra of 9H-A184C (measured with two samples) and 11 difference spectra of 9H-^{13}C-A184C (measured with three samples) has been used for SVD. The resulting first basis spectra represent the difference spectra in Figure 5, which have been taken to form the double difference. Simple averaging of the data has provided essentially the same results. The double difference spectrum shows only a positive band at 1645 cm^{-1} in the amide I region. In the amide II region, bands at 1543 cm^{-1} (−)/1532 cm^{-1}(+) and 1522 cm^{-1} (+)/1507 cm^{-1} (−) are observed. Though these isotope-induced bands are very small, they are found to be reproducible.

9H-F154C; 9H-S162C; 9H-S169C. Phenylanaline 154 is located at the cytoplasmic end of helix E, serine 169 is located in the cytoplasmic region of helix F, and serine 162 resides in the loop EF. Unequivocal bands could not be resolved in the respective double difference spectra (data not shown).

Discussion

Isotope-induced differences have been observed for the bacteriorhodopsin mutants T46C (helix B), L93C (helix C), and A184C (helix F). These residues are located in the middle to extracellular regions of the respective helices. It is clear that at these positions the backbone undergoes some conformational changes. For the mutants F154C (cytoplasmic end of helix E), S162C (loop EF), and S169C (cytoplasmic end of helix F), no isotope-induced spectral changes could be resolved. However, as long as the molecular cause for the amide I difference bands is not understood, it cannot be concluded that at these regions no conformational changes of the backbone take place. It is remarkable that for the mutants T46C and L93C, the largest changes occur at very high frequencies, well beyond the region of typical amide I bands of α-I/II helices.[42−44] This is probably due to the complicated coupling behavior of the C═O oscillators. Two questions have to be addressed: (1) What are the molecular causes for the amide I difference bands induced by the transition to a photointermediate? (2) How does isotope labeling influence the amide I difference bands?

In principle, the differences between the spectra of the labeled and unlabeled samples should reveal the original position of the bands caused by the initial and photoproduct states, as well as the corresponding shifted bands, the latter with opposite signs. If the corresponding mode is mainly determined by a single

C═O group, the shift should amount to approximately 37 cm^{-1}. It is clear that the observed isotopic spectral changes do not follow this scheme: for the T46C mutant (Figure 3), four bands, the 1692/1656 pair and the 1670/1631 pair, can be resolved exihibiting the expected isotopic shift. However, if this correlation would be correct, there would be two bands of the initial state, but no photoproduct bands (note that always the difference "labeled minus unlabeled" has been formed). For the L93C mutant (Figure 4), only one pair of bands is observed (1681/1641), again with the expected isotope shift. As before, it would correspond to the initial state. For the A184C mutant (Figure 5), only the band of the initial state can be discerned; the shifted one is missing. Thus, this simplified picture has to be modified.

Calculations of the amide absorption band of proteins and α-helical peptides may provide some hints for the interpretation.[9] Whereas the absoprtion band of an ideal α-helix shows only a few well-defined IR-active modes, the absorption spectra of a real peptide and of proteins exhibit a much wider distribution of amide I modes, even if the protein is mainly composed of α-helices as in the case of myoglobin. This is due to the coupling between the different structural units and also due to distortions of the ideal secondary structure. It has been recently shown that variations of the dihedral angles, deviating from the ideal structure, affect the amide I modes.[45] Thus, even if a half-width of only 2.5 cm^{-1} is used for each mode, broad amide I absorption bands are obtained.[46] This observation is corroborated by calculations concerning how isotopic labeling of a single peptide group within an α-helix influences the amide I absorption band:[7] the few IR-active modes of the ideal helix are split into a distribution of several modes, and new modes even appear at higher frequencies. Isotopic labeling of a single C═O oscillator represents a strong distortion of the coupling pattern by shifting the frequency. During the reaction of proteins, here bacteriorhodopsin, changes of the backbone structure may result in changes of the hydrogen bonding of C═O peptide groups altering the frequency and in changes of their orientations. Thus, it appears plausible that such distortions of the backbone can cause a pattern of difference bands with rather narrow half-width, also outside of the spectral range in which bands of the corresponding secondary structure are expected. Also, from the calculations on the spectral effects of isotopic labeling of a single peptide group,[7] it appears possible that the structural changes of a single peptide group can cause several difference bands. However, it is difficult to predict how such difference bands are additionally influenced by the isotopic labeling. In this connection, it is disadvantageous that the experimental determination of the isotopic effects, because of their small size, still bears considerable uncertainties: for the positions examined here, only the largest bands can be considered as reliable. Therefore, at present, these results only provide the local information that at these positions the backbone has been distorted by the photoreaction.

Isotope-induced alterations in the amide II region have also been, at least tentatively, identified by our studies. However, they are difficult to analyze because in the difference spectra the large bands caused by the ethylenic stretching vibration also determine the spectral features in this region. Thus, the unraveling of the small spectral differences induced by the isotopic substitution is even more hampered by the artifacts discussed above. Especially, intensity variations caused by detector nonlinearity[47] can severely influence the difference spectra, masking the isotope effects. In addition, the amide II mode has not been analyzed to the same extent as the amide I band. Therefore, it will not be further discussed.

How can the distortions of the backbone identified by our studies be related to the structural changes observed by other methods? Global structural changes occurring during the formation of the late M or of the N intermediate have been identified by low-resolution X-ray scattering experiments, identifying changes in the projection of the electron density on the purple membrane (see refs 48 and 49 and references therein). Such density changes are observed for helices B, F, and G, which can be interpreted in terms of tilting. More detailed information is obtained from spin-labeling experiments, which corroborate movements of the cytoplasmic part of helices C, F, and G[50,51] and even suggest a rotation of helix F.[52] As we have outlined in the Introduction, the rigid-body movement of the helices will not directly cause the narrow difference bands but rather cause broad absorption changes due to the infrared dichroic properties. However, it appears possible that these movements cause backbone distortions in the region of the hinges, which are supposed to be located in the middle or extracellular part of the helices. The distortions in this part of the helices B and F determined by us would be in agreement with such an interpretation. In view of these arguments, it is not surprising that no distortions have been detected for positions toward the cytoplasmic end of the helices because they are probably mainly involved in the rigid-body movement. Spin-label experiments have identified a reduced mobility of the label located at position 46 for the late M state. The corresponding amino acid in wild-type bacteriorhodopsin, T46, is connected to the proton donor for reprotonation of the Schiff base, D96, by a water molecule, and this proton channel is altered in the late M state (see ref 53 for a review). Thus, it appears possible that also the corresponding part of the backbone is influenced, as detected in our studies. Although movements of the EF-loop have been detected with the spin-label technique,[51] no isotope effect could be identified at position 162. Because in the loop region the peptide C═O groups are probably hydrogen-bonded to water molecules, such a movement would have a very small effect on the amide I band. Thus, so far our results are not in contradiction to the structural changes identified by other methods.

However, it should be mentioned that high-resolution structural analysis of the late M state of the D96N mutant has shown that the backbone of the cytoplasmic end of helix F, encompassing residues 162−179, has a considerably higher temperature factor than that in the dark state, which can only be explained by distortions of the helix. Thus, one would have expected that position 169, monitored by us, would be sensitive to these structural changes. Presently, there is no clear explanation for this discrepancy. It might be that the spectral changes are too small to be identified by our method.

Outlook

Future work will include systematic labeling of many more peptide oscillators within a complete helix giving more insights into the localization of the structural changes. Labeling of positions in helix G will be especially interesting because it can be expected that, because of the covalent link of the all-trans retinal chromophore to K216, the light-induced isomerization will especially affect helix G. Calculations of the amide I absorption bands based on the published high-resolution structures of the BR[16−20] and M states,[19,54] only taking the transition dipole coupling into account,[8] can be used to examine whether this approximation is capable of reproducing the observed amide I difference bands. Such calculations should include studies of the influence of isotopic labeling on the difference bands, which will provide a deeper insight into their molecular origin.

Acknowledgment. We are grateful to D. Oesterhelt and J. Riesle, Max-Planck-Institut für Biochemie, for the generous gift of the mutants used in this work. We also thank D. Oesterhelt and J. Tittor for helpful discussions. The work was supported by Fonds der Chemischen Industrie (to F.S.) and by the A.M.N. fund for the promotion of science, culture and arts in Israel and the Israel national science foundation (to M.S.). K.H. acknowledges a fellowship support from the ministry of science and culture Baden-Württemberg.

References and Notes

(1) Krimm, S.; Bandekar, J. *Adv. Protein Chem.* **1986**, *38*, 181−229.
(2) Mirkin, N. G.; Krimm, S. *J. Am. Chem. Soc.* **1991**, *113*, 9742−9747.
(3) Chen, X. G.; Schweitzer-Stenner, R.; Krimm, S.; Mirkin, N. G.; Asher, S. A. *J. Am. Chem. Soc.* **1994**, *116*, 11141−11142.
(4) Decatur, S. M.; Antonic, J. *J. Am. Chem. Soc.* **1999**, *121*, 11914−11915.
(5) Tadesse, L.; Nazarbaghi, R.; Walters, L. *J. Am. Chem. Soc.* **1991**, *113*, 7036−7037.
(6) Silva, R. A. G. D.; Kubelka, J.; Bour, P.; Decatur, S. M.; Keiderling, T. A. *Proc. Natl. Acad. Sci. U.S.A.* **2000**, *97*, 8318−8323.
(7) Brauner, J. W.; Dugan, C.; Mendelsohn, R. *J. Am. Chem. Soc.* **2000**, *122*, 677−683.
(8) Torii, H.; Tasumi, M. *J. Chem. Phys.* **1992**, *96*, 3379−3387.
(9) Torii, H.; Tasumi, M. *J. Chem. Phys.* **1992**, *97*, 86−91.
(10) Torii, H.; Tasumi, M. *J. Chem. Phys.* **1992**, *97*, 92−98.
(11) Hamm, P.; Lim, M. H.; Hochstrasser, R. M. *J. Phys. Chem. B* **1998**, *102*, 6123−6138.
(12) Wouterson, S.; Hamm, P. *J. Phys. Chem. B* **2000**, *104*, 11316−11320.
(13) Siebert, F. *Methods Enzymol.* **1995**, *246*, 501−526.
(14) Lanyi, J. K. *J. Biol. Chem.* **1997**, *272*, 31209−31212.
(15) Oesterhelt, D. *Curr. Opin. Struct. Biol.* **1998**, *8*, 489−500.
(16) Luecke, H.; Schobert, B.; Richter, H.-T.; Cartailler, J.-P.; Lanyi, J. K. *J. Mol. Biol.* **1999**, *291*, 899−911.
(17) Pebay-Peyroula, E.; Rummel, G.; Rosenbusch, J. P.; Landau, E. M. *Science* **1997**, *277*, 1676−1681.
(18) Mitsuoka, K.; Hirai, T.; Murata, A.; Miyazawa, A.; Kidera, A.; Kimura, Y.; Fujiyoshi, Y. *J. Mol. Biol.* **1999**, *286*, 861−882.
(19) Sass, H. J.; Büldt, G.; Gessenich, R.; Hehn, D.; Neff, D.; Schlesinger, R.; Berendzen, J.; Ormos, P. *Nature* **2000**, *406*, 649−653.
(20) Essen, L. O.; Siegert, R.; Lehmann, W. D.; Oesterhelt, D. *Proc. Natl. Acad. Sci. U.S.A.* **1998**, *95*, 11673−11678.
(21) Ludlam, C. F. C.; Sonar, S.; Lee, C. P.; Coleman, M.; Herzfeld, J.; RajBhandary, U. L.; Rothschild, K. J. *Biochemistry* **1995**, *34*, 2−6.
(22) Sonar, S.; Liu, X.; Lee, C. P.; Coleman, M.; He, Y. W.; Pelletier, S.; Herzfeld, J.; RajBhandary, U. L.; Rothschild, K. J. *J. Am. Chem. Soc.* **1995**, *117*, 11614−11615.
(23) Takei, H.; Gat, Y.; Rothman, Z.; Lewis, A.; Sheves, M. *J. Biol. Chem.* **1994**, *269*, 7387−7389.
(24) Steinhoff, H.-J.; Pfeiffer, M.; Rink, T.; Burlon, O.; Kurz, M.; Riesle, J.; Heuberger, E.; Gerwert, K.; Oesterhelt, D. *Biophys. J.* **1999**, *76*, 2702−2710.
(25) Engelhard, M.; Finkler, S.; Metz, G.; Siebert, F. *Eur. J. Biochem.* **1996**, *235*, 526−533.
(26) Blatz, P. E.; Lin, M.; Balasubramaniyan, P.; Balasubramaniyan, V.; Dewhurst, P. B. *J. Am. Chem. Soc.* **1969**, *91*, 5930−5931.
(27) Waddel, W. H.; Umerus, M.; West, J. L. *Tetrahedron Lett.* **1978**, *35*, 3223−3226.
(28) Tokunaga, F.; Ebrey, T. G. *J. Am. Chem. Soc.* **1978**, *17*, 1915−1922.
(29) Gerwert, K.; Siebert, F. *EMBO J.* **1986**, *5*, 805−811.
(30) Clark, N. A.; Rothschild, K. J.; Luippold, D. A.; Simon, B. A. *Biophys. J.* **1980**, *31*, 65−96.
(31) Fahmy, K.; Siebert, F.; Tavan, P. *Biophys. J.* **1991**, *60*, 989−1001.
(32) Weidlich, O.; Friedman, N.; Sheves, M.; Siebert, F. *Biochemistry* **1995**, *34*, 13502−13510.
(33) Delaney, J. K.; Schweiger, U.; Subramaniam, S. *Proc. Natl. Acad. Sci. U.S.A.* **1995**, *92*, 11120−11124.
(34) Subramaniam, S.; Greenhalgh, D. A.; Rath, P.; Rothschild, K. J.; Khorana, H. G. *Proc. Natl. Acad. Sci. U.S.A.* **1991**, *88*, 6873−6877.
(35) Halverson, K. J.; Sucholeiki, I.; Ashburn, T. T.; Lansbury, P. T., Jr. *J. Am. Chem. Soc.* **1991**, *113*, 6701−6703.
(36) Malinowski, E. R. *Factor Analysis in Chemistry*, 2nd ed.; John Wiley & Sons: New York, 1991.
(37) Delaney, J. K.; Schweiger, U.; Subramaniam, S. *Proc. Natl. Acad. Sci. U.S.A.* **1995**, *92*, 11120−11124.
(38) Sulkes, M.; Lewis, A.; Marcus, M. A. *Biochemistry* **1978**, *17*, 4712−4721.
(39) Heyde, M. E.; Gill, D.; Kilponen, R. G.; Rimai, L. *J. Am. Chem. Soc.* **1971**, *93*, 6776−6780.
(40) Callender, R.; Honig, B. *Annu. Rev. Biophys. Bioeng.* **1977**, *6*, 33−55.
(41) Pfefferle, J. M.; Maeda, A.; Sasaki, J.; Yoshizawa, T. *Biochem.* **1991**, *30*, 6548−6556.
(42) Wang, J.; El-Sayed, M. A. *Biophys. J.* **1999**, *76*, 2777−2783.
(43) Krimm, S.; Dwivedi, A. M. *Science* **1982**, *216*, 407−408.
(44) Gibson, N. J.; Cassim, J. Y. *Biochemistry* **1989**, *28*, 2134−2139.
(45) Torii, H.; Tasumi, M. *J. Raman Spectrosc.* **1998**, *29*, 81−86.
(46) Torii, H.; Tasumi, M. In *Infrared Spectroscopy of Biomolecules*; Mantsch, H. H., Chapman, D., Eds.; Wiley-Liss, Inc.: New York, 1996; Chapter 1, pp 1−18.
(47) Rödig, C.; Siebert, F. *Fourier Transform Spectroscopy: 11th International Conference*; de Haseth, J. A., Ed.; American Institute of Physics: Woodbury, New York, 1998; Chapter 430, pp 388−391.
(48) Sass, H. J.; Schachowa, I. W.; Rapp, G.; Koch, M. H. J.; Oesterhelt, D.; Dencher, N. A.; Büldt, G. *EMBO J.* **1997**, *16*, 1484−1491.
(49) Kamikubo, H.; Kataoka, M.; Váró, G.; Oka, T.; Tokunaga, F.; Needleman, R.; Lanyi, J. K. *Proc. Natl. Acad. Sci. U.S.A.* **1996**, *93*, 1386−1390.
(50) Radzwill, N.; Gerwert, K.; Steinhoff, H.-J. *Biophys. J.* **2001**, *80*, 2856−2866.
(51) Rink, T.; Pfeiffer, M.; Oesterhelt, D.; Gerwert, K.; Steinhoff, H.-J. *Biophys. J.* **2000**, *78*, 1519−1530.
(52) Xiao, W.; Brown, L. S.; Needleman, R.; Lanyi, J. K.; Shin, Y.-K. *J. Mol. Biol.* **2000**, *304*, 715−721.
(53) Brown, L. S. *Biochim. Biophys. Acta* **2000**, *1460*, 49−59.
(54) Luecke, H.; Schobert, B.; Richter, H.-T.; Cartailler, J.-P.; Lanyi, J. K. *Science* **1999**, *286*, 255−260.